International Journal of Nanomedicine

Dovepress
open access to scientific and medical research

Open Access Full Text Article

ORIGINAL RESEARCH

Peripheral Serum Exosomes Isolated from Patients with Acute Myocardial Infarction Promote Endothelial Cell Angiogenesis via the miR-126-3p/TSC1/mTORC1/HIF-1α Pathway

Shasha Duan[1–3,*], Chao Wang[1,2,*], Xiangli Xu[4], Xiaoshan Zhang[3], Gaofeng Su[1,2], You Li[1,2], Shuai Fu[1,2], Ping Sun[1,2], Jiawei Tian[1]

[1]Department of Ultrasound, the Second Affiliated Hospital of Harbin Medical University, Harbin, Heilongjiang Province, People's Republic of China; [2]The Key Laboratory of Myocardial Ischemia, Harbin Medical University, Ministry of Education, Harbin, Heilongjiang Province, People's Republic of China; [3]Department of Ultrasound, The Affiliated Hospital of Inner Mongolia Medical University, Hohhot, People's Republic of China; [4]Department of Ultrasound, the Second Hospital of Harbin city, Harbin, Heilongjiang Province, People's Republic of China

*These authors contributed equally to this work

Correspondence: Jiawei Tian; Ping Sun, Department of Ultrasound, the Second Affiliated Hospital of Harbin Medical University, No. 246 Xuefu Road, Nangang District, Harbin, Heilongjiang Province, 150086, People's Republic of China, Tel +86 451-86605811, Fax +86 451-86605745, Email jwtian2004@163.com; sunpinghmu@163.com

Purpose: Angiogenesis is required for improving myocardial function and is a key factor in long-term prognosis after an acute myocardial infarction (AMI). Although exosomes are known to play a crucial role in angiogenesis, the role of peripheral exosomes in angiogenic signal transduction in patients with AMI remains unclear. Here, we explored the effect of exosomes extracted from the peripheral serum of AMI patients on angiogenesis and elucidated the downstream pathways.

Patients and Methods: Serum exosomes were obtained from patients with AMI (AMI-Exo) and healthy individuals (Con-Exo). The exosomes were cocultured with human umbilical vein endothelial cells (HUVECs) in vitro, with aortic rings ex vivo, and were used to treat mouse hind-limb ischemia and mouse AMI model in vivo.

Results: AMI-Exo raised HUVEC proliferation, tube formation, and migration, and enhanced microvessel sprouting from aortic rings compared to Con-Exo, both in vitro and ex vivo. Quantitative reverse transcription-polymerase chain reaction revealed that the abundance of miR-126-3p, a crucial regulator of angiogenesis, was increased in AMI-Exo. The inhibition of miR-126-3p decreased the benefits of AMI-Exo treatment, and miR-126-3p upregulation enhanced the benefits of Con-Exo treatment in HUVECs, aortic rings, the mouse hind-limb ischemia model, and the mouse AMI model. Knockdown and overexpression analyses revealed that miR-126-3p regulated angiogenesis in HUVECs by directly targeting tuberous sclerosis complex 1 (TSC1). Moreover, we found that miR-126-3p could inhibit TSC1 expression, which further activated mTORC1 signaling and increased HIF-1α and VEGFA expression, ultimately promoting angiogenesis.

Conclusion: Collectively, our results provide a novel understanding of the function of exosomes in angiogenesis post AMI. We demonstrated that exosomes from the peripheral serum of AMI patients promote angiogenesis via the miR-126-3p/TSC1/mTORC1/HIF-1α signaling pathway.

Keywords: acute myocardial infarction, angiogenesis, exosomes, miR-126-3p, tuberous sclerosis complex 1

Introduction

Cardiovascular diseases (CVDs) pose immense health and economic burdens worldwide, and account for 44% of all disease-related deaths in China.[1] Acute myocardial infarction (AMI) is the leading cause of death from CVDs. Although thrombolytic anticoagulant therapy and percutaneous coronary intervention can largely restore occluded coronary perfusion after AMI, they cannot repair the damage caused to microvascular architecture in ischemic myocardium by

Received: 12 September 2021
Accepted: 7 March 2022
Published: 2 April 2022

coronary hypoxic ischemia. Angiogenesis is a complex process of vascular endothelial cell proliferation, migration, and branching that forms new microvessels from existing vessels in response to various factors. Since angiogenesis plays an important role in improving myocardial function after AMI,[2] it is necessary to explore the underlying mechanisms and identify effective new therapeutic targets.

Exosomes are a type of extracellular microvesicle, with diameters ranging from 30 nm to 150 nm. They contain all kinds of functional biomolecules (DNA, mRNAs, lipids, proteins, and microRNAs [miRNAs]) that can be transferred to nearby or distant cells via the circulatory system.[3] Previous studies have shown that plasma exosomes derived from adult rats and humans can protect the myocardium from ischemia-reperfusion injury by delivering endogenous protective signals to the myocardium.[4] In addition, it has been reported that cardiomyocytes from mice with ischemic injury may release cell-dependent exosomes into the circulatory system.[5] During transport, exosomes can protect bioactive molecules from degradation.[6] For instance, Cao et al[7] reported that during AMI convalescence, circulating exosomes can be transported between cells through dynamin, and transport miR-193a-5p to protect endothelial cells experiencing oxidative stress. However, it remains unclear whether exosomes derived from the circulatory serum during early phases of AMI can play regulatory roles in endothelial cell angiogenesis.

In this study, we researched the function of circulating exosomes in angiogenesis; the exosomes were isolated from AMI patients within 12 h of clinical symptom onset (AMI-Exo) and healthy individuals (Con-Exo). The function of human umbilical vein endothelial cell (HUVEC), microvessel sprouting from aortic rings in ex vivo, and the hind limb ischemia as well as AMI mouse model were studied. Taken together, our findings can provide new targets for research into the mechanisms of angiogenesis during myocardial infarction.

Patients and Methods

Patients

The diagnostic criteria for AMI patients were according to the 2012 ESC/AHA/ACC guidelines.[8] The study participants were patients with suspected AMI based on electrocardiographic diagonal evidence, chest pain, and diagnostic cardiac catheterization at the Second Affiliated Hospital of Harbin Medical University between May 2018 and July 2019. The exclusion criteria were: 1) diabetes, 2) infectious diseases, and 3) other contraindications including tumors and nephritic or hepatic diseases. According to their angiography results, patients with more than 70% stenosis of the coronary artery were treated as the AMI group. Healthy individuals served as the control group. All individuals signed informed consent and the experiments were approved by the Second Affiliated Hospital of Harbin Medical University Ethics Committee (Harbin City, Heilongjiang Province, China). This experiment was conducted in accordance with the Declaration of Helsinki.

Serum Exosome Preparation and Identification

Blood samples (10 mL) were collected from the peripheral veins of all research subjects. From the AMI patients, the blood samples were collected before coronary stent implantation and within 12 h of the onset of chest pain. Serum exosomes were isolated from all subjects as described previously.[9] Briefly, the serum samples were centrifuged at 1000 × g for 5 min and again at 10,000 × g for 10 min. Then, a 0.1 mm pore mesh was used to filter the cells; these were then ultracentrifuged at 100,000 × g for 1h. The exosomes were washed by PBS and subjected once again to ultracentrifugation at 100,000 × g for 1 h. The derived microvesicles were resuspended in PBS for later experiments. Bicinchoninic acid (BCA) protein kit (Beyotime, Shanghai, China) was used to quantitatively evaluate the exosome concentration. The size distribution and ultrastructure of the exosomes were analyzed using nanoparticle tracking analysis (NTA) and transmission electron microscopy (TEM; H-7650; Hitachi, Japan); their Alix, CD63, and TSG101 expression were analyzed using Western blotting.

Cell Culture

HUVECs obtained from Type Culture Collection of the Chinese Academy of Sciences, Shanghai, China, were employed. The cells were cultured using Dulbecco modified eagle medium (DMEM) (Gibco, BRL, USA), 10% newborn calf serum (Invitrogen Life Technologies, Carlsbad, California, USA), and 1% penicillin-streptomycin (Beyotime, Shanghai, China). The culture plates were placed in an environment with the following conditions: temperature: 37°C, O_2: 21%, and CO_2: 5%.

Experimental Animals

Wild-type male 8–9-week-old C57BL/6 mice and 6-week-old Sprague–Dawley rats were purchased from the Medical Laboratory Animal Supply Base (Heilongjiang, China). The animals were reared in accordance with the principles of animal care approved by the National Society for Medical Research and the Guideline for the Care and Use of Laboratory Animals (Institute of Laboratory Animal Resources/NIH). The experiments on animals were allowed by the Research Ethics Committee of the Second Affiliated Hospital of Harbin Medical University (SYDW2020-030).

Quantitative RT-PCR Analysis

Exosomal RNA was derived from exosomes using a miRcute miRNA Isolation Kit (Tiangen Biotech, Beijing, China) and then reverse transcribed into cDNA using an miRcute Plus miRNA First-Strand cDNA Synthesis Kit (Tiangen Biotech), based on standard protocols. Total cellular RNA was extracted by TRIzol reagent (Invitrogen) and mRNA was reverse transcribed using a Transcriptor First Strand cDNA Synthesis Kit (Roche Diagnostics, Risch-Rotkreuz, Switzerland). For exosomal miRNA, the relative levels were normalized compared to those of synthetic *Caenorhabditis elegans* (cel)-miR-39 (5 fmol/mL; Applied Biosystems, California, USA). Meanwhile, for cellular miRNA, relative levels were normalized with U6 RNA. Cellular mRNA levels were normalized to GAPDH mRNA standards. Quantitative analysis was conducted using the $2^{-\Delta\Delta Ct}$ method. The primers are shown in Table S1.

Western Blotting Analysis

Sodium dodecyl sulfate polyacrylamide gel electrophoresis (SDS-PAGE) was used to separate proteins; these were then transferred onto polyvinylidene difluoride membranes (Millipore, Massachusetts, USA), and incubated at 4 °C overnight together with primary antibodies against Alix (Abcam, ab186429, UK), CD63 (Abcam, ab217345), TSG101 (Abcam, ab125011), TSC1 (CST, 6935, China), HIF-1α (Abcam, ab179483), phospho-S6 S240/244 (CST, 5364), S6 (CST, 2217), VEGFA (Abcam, ab214424), and GAPDH (Bioss, Beijing, China). Secondary antibodies were purchased from (Zsbio, Beijing, China). The expression of the genes in the samples were normalized to that of GAPDH.

HUVEC Proliferation, Tube Formation, and Migration

HUVEC proliferation was evaluated using Cell Counting kit-8 (Dojindo, CK04-11, Japan), Cell-Light EdU (5-ethynyl-2′-deoxyuridine) kit (Ribobio, C10310-3, Guangzhou, China), and manual cell counting assay. Briefly, 100 μL of cell suspension including approximately 3000 HUVECs was placed in a 96-well plate and treated with 200 μg/mL AMI-Exo, Con-Exo, and PBS, respectively. After 24 h, CCK-8 reagent (10 μL) was added and the cells were cultivated for 3 h. Then, spectrophotometric microplate reader was used for measuring the optical density (OD) at 450 nm. In the EdU assay, the labelling reagent was added to a 96-well plate and the HUVECs were allowed to proliferate for 2 h. The cells were imaged using a fluorescence microscope (Leica, Germany).

HUVEC migration was analyzed using Transwell inserts (Corning, 3422, USA) and scratch wound assays. Cells were resuspended in serum-free DMEM, dispensed in the Transwell inserts (approximately 2×10^5 cells/well); the cells then migrated to the underside containing DMEM with 10% FBS, through the 8.0 μm pore polycarbonate membrane. The cells were then treated with PBS, Con-Exo, AMI-Exo, and cultured for 8 h at 37°C with 5% CO_2. Cells within each insert were removed using cotton swabs. The migrated cells were treated with crystal violet for 10 min and quantitated in three random microscopic fields.

Scratch wound assays were carried out by resuspending HUVECs seeded in 6-well plates and starving them for 12h. A scratch wound was created using a yellow pipette tip and then, PBS, Con-Exo or AMI-Exo were added, respectively. After 24 h, the wound area was observed and analyzed by ImageJ software. The ratio of non-migrated area divided by the baseline area was used to calculate the migration effects.

In in-vitro tube formation assay, 50 μL Matrigel Matrix (BD, 356234) was added to a 96-well plate. Then, about 2×10^4 cells/well were seeded on the Matrigel and co-cultured with PBS, Con-Exo, or AMI-Exo for 8 h. The total tube length and number of nodes were quantitatively analyzed by ImageJ software.

Aortic Ring Assay

All procedures were performed under sterile conditions. Briefly, 1 mL Matrigel Matrix (BD, 356234) was mixed with serum-free medium 1:1 in a 2.5 mL Eppendorf (EP) tube, added to a 96-well plate (70 μL/well), and incubated at 37 °C for 30 min. Six-week old Sprague–Dawley rats were euthanized and their thoracic aorta dissected. After the removal of the surrounding tissue and fat, the aorta was cut into ~1 mm sections. One ring was gently placed in each well of a 96-well plate with 70 μL mixed Matrigel in serum-free medium 1:1, and incubated at 37 °C. Ring sprouting was visualized on day 4 using a light microscope with a phase-contrast setting. Sprout outgrowths were counted manually. The number of sprouts that emerged from the main ring as well as the individual branches arising from it as separate vessels were counted.[10]

Luciferase Assay

Overlap analysis revealed that TSC1 may be a potential therapeutic target. Wild-type and mutated *TSC1* mRNA 3′ UTR fragments were synthesized and inserted into the p-MIR-REPORT plasmid (GenePharma, Shanghai, China). The 293T cells were co-transfected with 60 nM of mimic miR-126-3p or inhibitor and 10 ng of *Renilla* luciferase reporter. After 24 h, *Renilla* luciferase activity was evaluated by Dual-Luciferase Reporter Assay System (Promega, USA), based on the manufacturer's protocol.

Statistical Analysis

Continuous variables were presented as the mean ± standard deviation or as the median and interquartile range. Student's *t*-test or Mann–Whitney *U*-test, as appropriate. Categorical variables were expressed as numbers and percentages, and analyzed using the chi-square test. The SPSS statistical software (version 25.0; SPSS Inc., IBM Corp., Armonk, NY, USA) was employed. Two-sided *P* values of < 0.05 were considered as statistically significant. Histograms were drawn using GraphPad Prism 8.0 (GraphPad Software, California, USA).

Further information on the methods is described in the Supplementary Information.

Results

Serum Exosome Characterization

Twenty AMI patients and 10 healthy individuals were included in this study. Their clinical baseline characteristics are shown in Table 1. Serum exosomes from the healthy individuals and AMI patients were derived by ultracentrifugation, as reported previously,[11] and their morphology was analyzed using TEM. The exosomes displayed a round, cup-shaped morphology (Figure 1A). Specific exosomal markers (Alix, CD63, and TSG101) were expressed in both exosome types (Figure 1B), and NanoSight measurement showed that they both displayed particle size distributions of 30–150 nm (Figure 1C). Meanwhile, there was no statistical difference in concentration between Con-Exo and AMI-Exo (Figure 1D). Taken together, these results confirm that exosomes were the main components of the purified microvesicles.

Serum-Derived Exosomes Were Internalized Well by Endothelial Cells

To explore whether the exosomes can be internalized by endothelial cells, we incubated PKH67-stained exosomes with HUVECs for 24 h; > 90% of HUVECs were found to be positive for PKH67 fluorescence, with no difference between the internalization of AMI-Exo and Con-Exo (Figure 1E). Confocal imaging confirmed that the exosomes were effectively internalized by the HUVECs (Figure 1F). Thus, the isolated exosomes could be internalized by endothelial cells.

AMI-Exos Promote Angiogenesis in vitro and ex vivo

To explore the functions of the exosomes acting on endothelial cells, HUVECs were co-cultured with exosomes isolated from both (control and AMI) groups. AMI-Exo promoted HUVEC proliferation to a greater extent than Con-Exo after treatment, as revealed by EdU and CCK8 assays (Figure 2A-C) and confirmed by manual cell counting (Figure 2D). Vascular formation effect was evaluated using Matrigel assays, which showed that AMI-Exo augment the total tube length and number of nodes compared to Con-Exo, indicating that they possess higher pro-angiogenic abilities (Figure 2E-G). To assess the migration of cells after exosome treatment, we also performed Transwell and scratch

Table 1 The Baseline Characteristics of AMI Patients and Healthy Persons

Characteristics	AMI (n = 20)	Control (n = 10)	*P*
Age (year)	58 ± 12	65 ± 14	0.134[a]
Male (%)	65	80	0.675[b]
Smoking (%)	85	30	0.003[b]
Glucose (mmol/L)	4.99 ± 0.96	5.41 ± 0.67	0.236[a]
Cholesterol (mmol/L)	1.66 (1.05 to 4.23)	1.35 (1.15 to 1.69)	0.397[c]
Triglyceride (mmol/L)	1.12 (1.02 to 1.34)	0.79 (0.54 to 1.08)	0.019[c]
HDL(mmol/L)	2.41 ± 1.14	3.01 ± 0.43	0.048[a]
LDL(mmol/L)	2.96 ± 0.54	1.92 ± 0.28	<0.001[a]
cTnI (ug/L)	29.25 (3.91 to 110.13)	–	
Hypertension (%)	75	20	0.004[b]
Characteristics of lesion			
LAD (%)	80	–	
LCX (%)	60	–	
RCA (%)	35	–	
LV dysfunction (%)	55	–	

Notes: [a]*P*-value by *t*-test. [b]*P*-value by chi-squared test. [c]*P*-value by Mann–Whitney *U*-test.
Abbreviations: AMI, Acute myocardial infarction; LDL, low density lipoprotein; HDL, high density lipoprotein; cTnI, cardiac troponin I; LAD, left anterior descending coronary artery; LCX, left circumflex artery; RCA, right coronary artery.

wound assays. AMI-Exo exerted greater effects than Con-Exo on both the migration area in the wound assay (Figure 2H and I) and the migrated cell number in the Transwell assay (Figure 2J and K). To further investigate the pro-angiogenic properties of the AMI exosomes, we performed aortic ring assays, which revealed that conditioned media contained

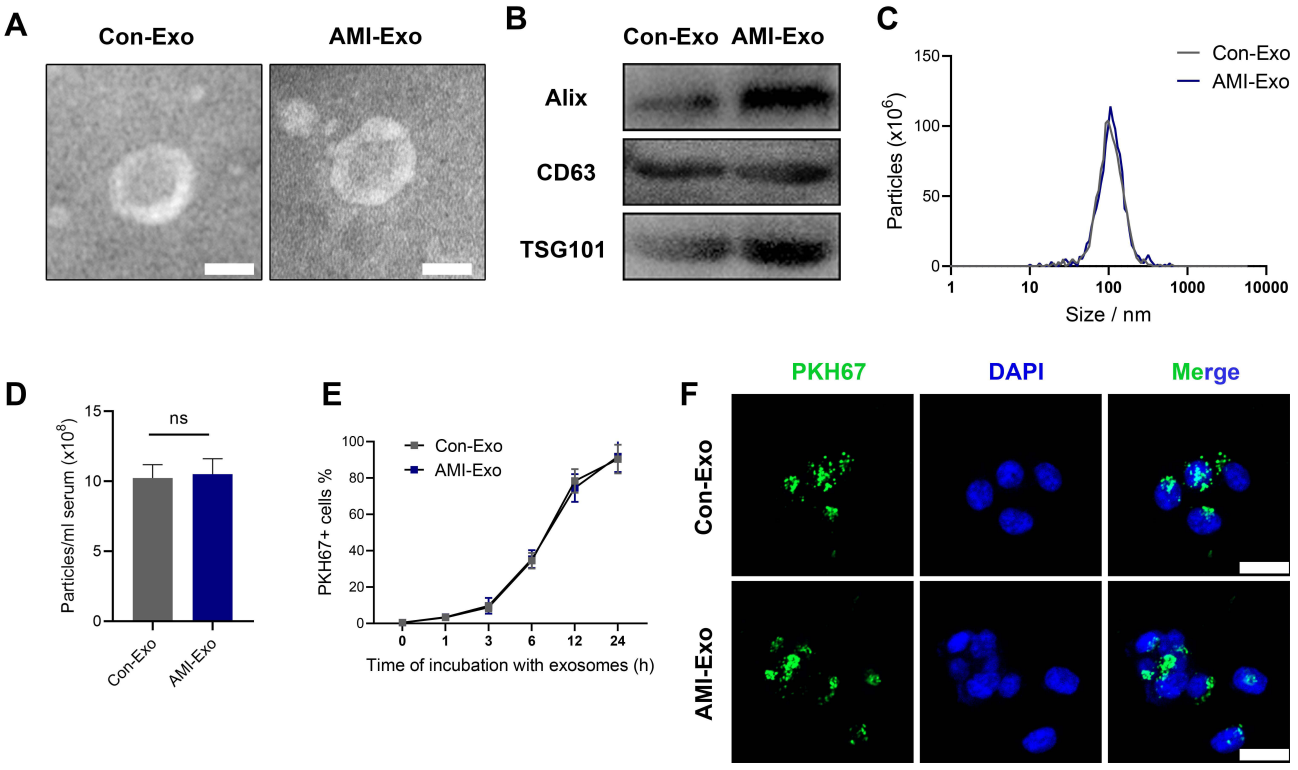

Figure 1 Exosome characterization and internalization pathways. (**A**) Transmission electron microscopy images of exosomes isolated from the two groups. Scale bar, 100 nm. (**B**) Protein expression of the exosomal markers Alix, CD63, and TSG101. (**C**) Exosome particle diameter distribution. (**D**) The concentration of exosome between control group and AMI individuals. (**E**) Exosome uptake was analyzed at the indicated times using flow cytometry. (**F**) Exosome uptake in human umbilical vein endothelial cells (HUVECs) incubated with PKH67-labeled exosomes (green), as analyzed by confocal imaging. Nuclei were dyed with DAPI (blue). Scale bar, 20 μm.

AMI-Exo markedly enhanced microvessels sprouting from aortic rings (Figure 2L and M). Overall, results of our in vitro and ex vivo assays showed that both Con-Exo and AMI-Exo could promote angiogenesis compared with PBS group. However, AMI-Exo exerted greater effects than Con-Exo in angiogenesis-related procedures, including proliferation, tube formation, migration, and microvessel sprouting, suggesting that exosomes from the peripheral serum of patients with AMI may contain certain angiogenic signals than those from healthy individuals.

miR-126-3p Expression is Up-Regulated in AMI-Exo

Recent studies have demonstrated that exosomes exert crucial effects in different cell types via miRNA transport. To investigate the mechanisms underlying the angiogenic roles of the exosomes, we chose several angiogenesis-related miRNAs (miR-143, miR-17-5p, miR-21-5p, miR-939-5p, and miR-126-3p),[5,12–15] and validated their differential expression in the serum exosomes of AMI patients and control individuals using qRT-PCR. miR-126-3p expression differed significantly between the two groups, indicating that circulating AMI-Exos may load miR-126-3p (Figure 3A-E). Next, HUVECs were incubated with exosomes and RNA polymerase II inhibitor. The results showed that there was no significant difference in the miR-126-3p expression between the two groups (Figure 3F), suggesting that AMI-Exo did not induce endogenous miR-126-3p transcription in HUVECs. The effect induced by miR-126-3p, thus was attributed to exosome transport.

miR-126-3p from AMI-Exo Promotes Angiogenesis in vitro and ex vivo

To verify that miR-126-3p is essential for the exosomal regulation of angiogenesis in vitro and ex vivo, we co-cultured HUVECs and aortic rings with PBS, Con-Exo + mimic NC, Con-Exo + mimic miR-126-3p, AMI-Exo + inhibitor NC, and AMI-Exo + inhibitor miR-126-3p. Con-Exo + mimic miR-126-3p and AMI-Exo + inhibitor NC promoted endothelial cell proliferation better than Con-Exo + mimic NC and AMI-Exo + inhibitor, respectively, as indicated by CCK8 and Edu analyses (Figure 4A-D). In addition, Matrigel assays to assess vascular formation ability revealed that Con-Exo transfected with the miR-126-3p increased the number of nodes and total tube length, whereas AMI-Exo transfected with the inhibitor miR-126-3p decreased AMI-Exo induced vascular formation, suggesting that exosomal miR-126-3p exerts pro-angiogenic effects post AMI (Figure 4E-G). We also performed Transwell and scratch wound assays to evaluate the migration of cells considering the four types of exosomes. Notably, exosomal miR-126-3p transfection promoted cell migration in wound assay (Figure 4H and I) and increased the number of migrated cells in Transwell assay (Figure 4J and K). While, exosomal inhibitor miR-126-3p transfection abolished the effects of AMI-Exo promoted HUVEC migration (Figure 4H-K). Furthermore, conditioned media contained Con-Exo + mimic miR-126-3p or AMI-Exo + inhibitor NC markedly enhanced microvessel sprouting from aortic rings (Figure 4L and M). Together, these findings indicate that miR-126-3p in AMI-Exos plays a key role in angiogenesis.

miR-126-3p from AMI-Exo Promotes Angiogenesis in Mouse Hind Limb Ischemia

To further investigate the angiogenic effects of miR-126-3p from AMI-Exo and Con-Exo in vivo, we generated a mouse model of unilateral hind limb ischemia that was injected intramuscularly with PBS or exosomes on day 1 after surgery. As per a previous study,[5] exosomes were diluted in PBS. Then, we injected 200μL different concentration AMI-Exo, as 5×10^2 μg/mL, 1×10^3 μg/mL, 2×10^3 μg/mL, or PBS on day 1 after surgery. We found that the exosomal concentration of approximately 1×10^3 μg/mL in 200 μL PBS was the optimal amount (Figure S1). Thus, this amount was chosen for the following experiments. qRT-PCR assays revealed a high miR-126-3p expression in the muscles treated with Con-Exo + mimic miR-126-3p and AMI-Exo + inhibitor NC (Figure 5A). No significant differences in blood flow recovery were observed between the four groups 3 and 7 days post-treatment; however, the Con-Exo + mimic miR-126-3p and AMI-Exo + inhibitor NC groups showed significantly higher blood perfusion 14 days post-injection than the Con-Exo + mimic NC and AMI-Exo + inhibitor miR-126-3p groups, respectively (Figure 5B and C). The gastrocnemius muscles were harvested, embedded, sectioned, and subjected to H&E staining (Figure 5D) and immunofluorescence (Figure 5E). Angiogenesis after ischemia was detected using the vascular marker CD31 and α-SMA. The groups treated with Con-Exo + mimic miR-126-3p and AMI-Exo + inhibitor NC showed a significantly higher capillary density than those treated with Con-Exo + mimic NC and AMI-Exo + inhibitor miR-126-3p (Figure 5F), respectively, indicating

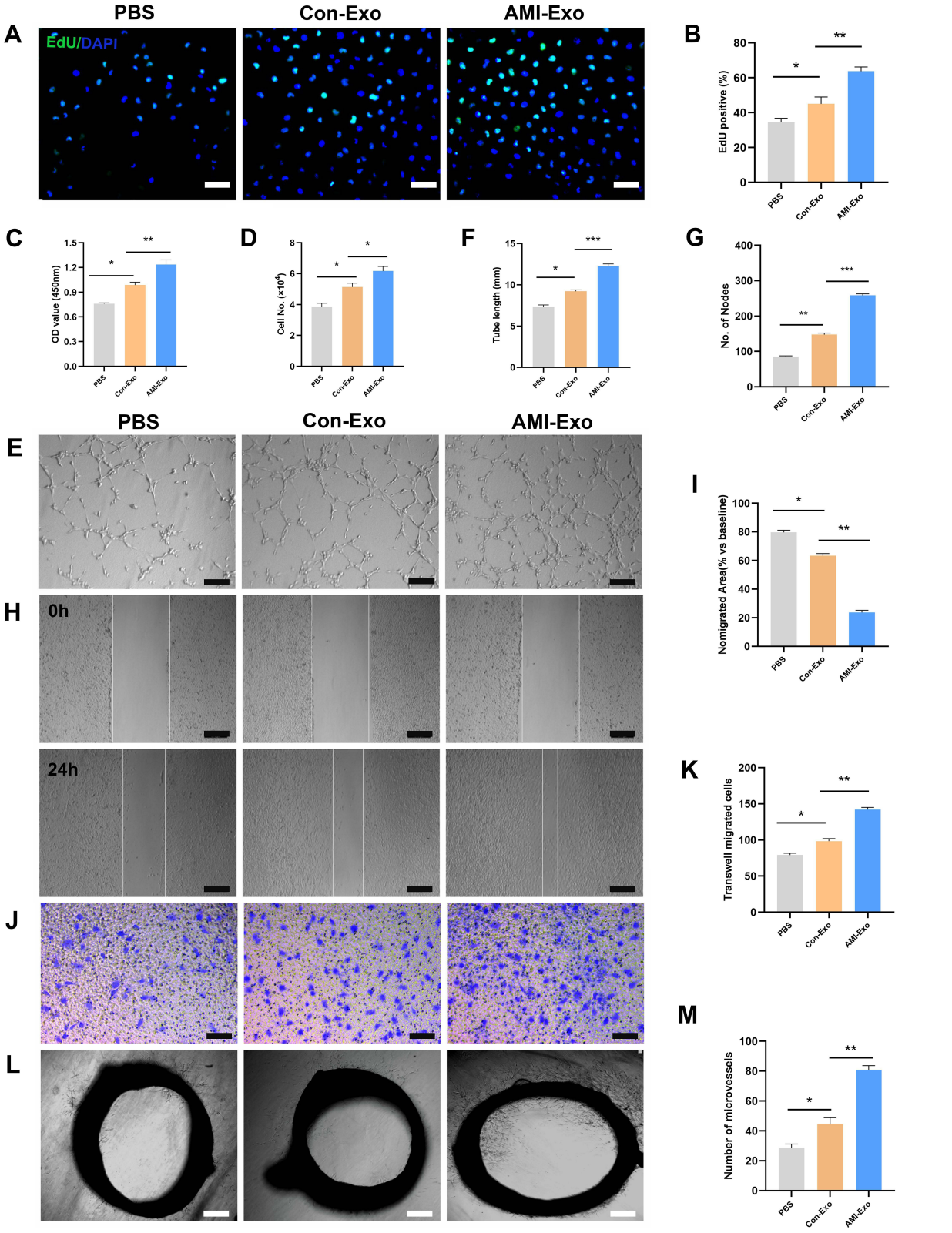

Figure 2 Effects of AMI-Exo and Con-Exo treatment on angiogenesis in vitro and ex vivo. (**A** and **B**) Proliferation of EdU-positive HUVECs, as evaluated by CCK8 (**C**) and manual cell counting (**D**). Scale bar, 50 μm. (**E**) Tube formation analysis of vascular formation ability, as measured by tube length (**F**) and node number (**G**). Scale bar, 100 μm. Cell migration was quantitated using scratch wound assays (**H**) and the ratio of the non-migrated area divided by the baseline wound area was analyzed (**I**). Scale bar, 100 μm. Cell migration was analyzed using Transwell assays (**J** and **K**). Scale bar, 50 μm. (**L**) Aortic sprouting assays were used to quantify the number of microvessels (**M**). Scale bar, 200 μm. *$p < 0.05$, **$p < 0.01$, ***$p < 0.001$.

https://doi.org/10.2147/IJN.S338937 DovePress

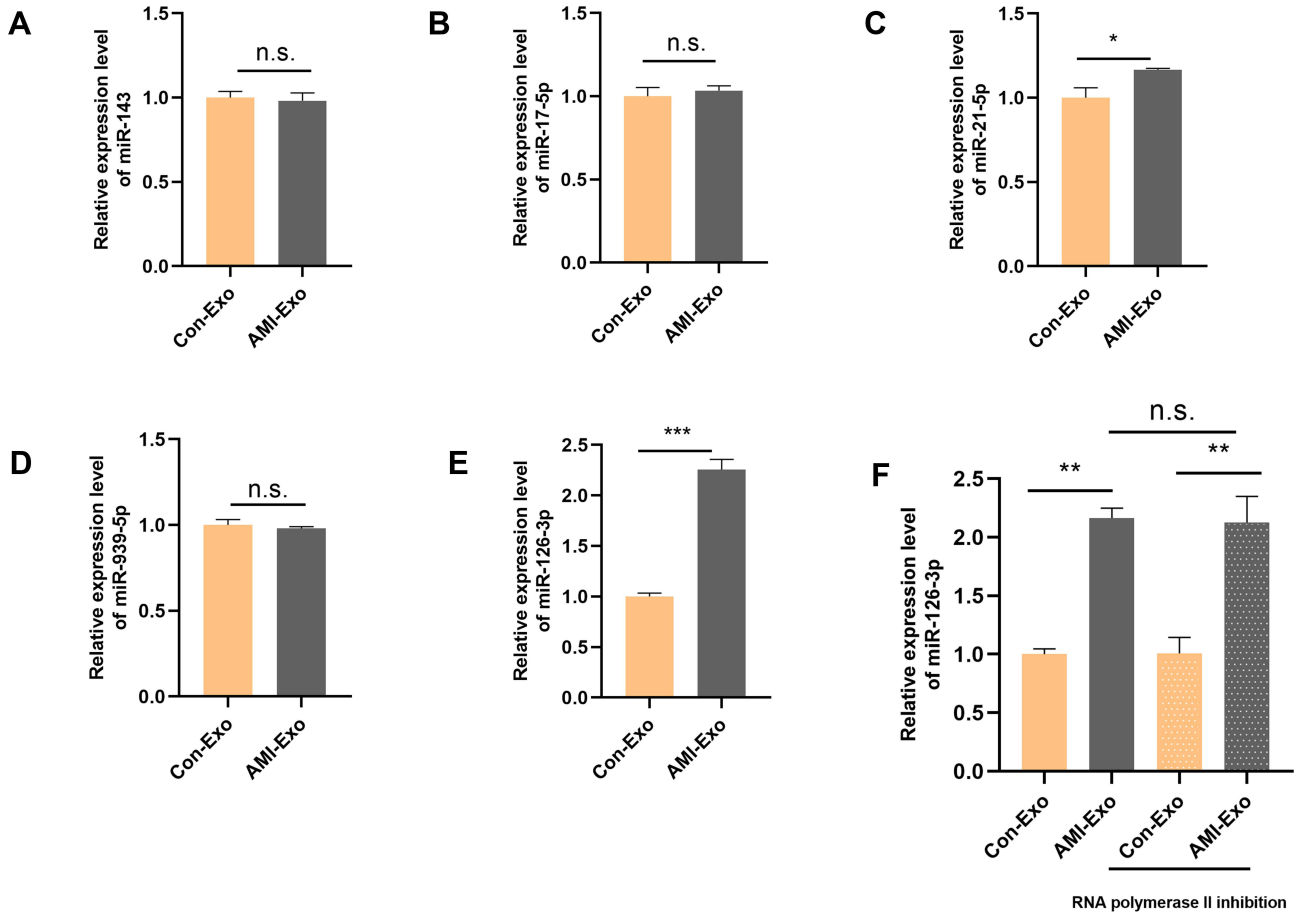

Figure 3 Peripheral serum exosomes from AMI patients were loaded with miR-126-3p. (**A**–**E**) The expression level of angiogenesis-related miRNAs in exosomes isolated from the two groups was evaluated using qRT-PCR. (**F**) Exosomes were added to HUVECs with or without an inhibitor of RNA polymerase II transcription (5,6-dichloro-1-b-D-ribofuranosylbenzimidazole). After treatment for 24 h, miR-126-3p levels in the HUVECs were analyzed. *$p < 0.05$, **$p < 0.01$, ***$p < 0.001$.

that exosomal miR-126-3p may play a key role in microvascular construction. Overall, these analyses of the mouse hind limb ischemia model showed that miR-126-3p in peripheral serum-derived exosomes promotes post-ischemic recovery.

miR-126-3p from AMI-Exo Promotes Angiogenesis in Mouse AMI Model

To further investigate the angiogenic effects of exosomal miR-126-3p in mouse AMI model, we intramyocardially injected PBS or exosomes into the left ventricular wall (border zone) immediately after the left anterior descending ligation. The cardiac tissue was collected 14 days after the myocardial infarction. The qRT-PCR assays revealed that the miR-126-3p-enriched exosomes could effectively deliver miR-126-3p to the myocardium (Figure 6A). The immunohistochemical assay was performed to assess angiogenesis after ischemia by detecting the number of vessels. Con-Exo + mimic miR-126-3p group showed a significantly higher capillary density than Con-Exo + mimic NC group. The AMI-Exo + inhibitor miR-126-3p group showed a significantly lower capillary density than AMI-Exo + inhibitor NC group (Figure 6B–D). Collectively, these analyses of the mouse AMI model showed that miR-126-3p in peripheral serum-derived exosomes promotes post-ischemic endothelial cell angiogenesis.

miR-126-3p Promotes Endothelial Cell Angiogenesis by Targeting TSC1 and Activates the mTORC1/HIF-1α Signaling Pathway

Mutations in TSC1 or TSC2 have been reported to lead to benign malformations or tumors, such as lymphangioleiomyomatosis and angiomyolipoma, in several different organs.[16] Therefore, TSC1 may play important roles in

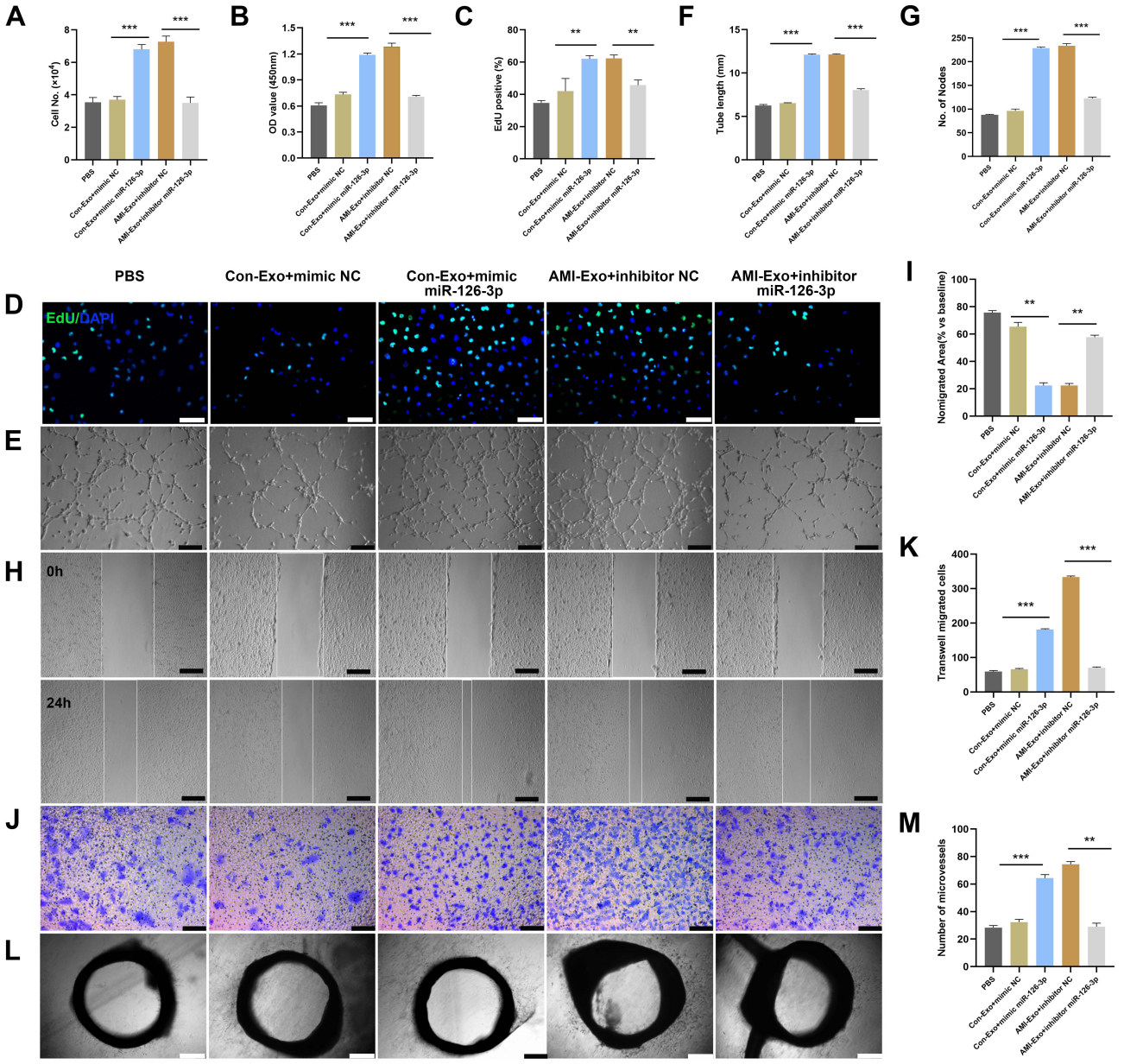

Figure 4 miR-126-3p in AMI-Exo promotes angiogenesis in vitro and ex vivo. Mimic miR-126-3p and inhibitor or control (NC) were transfected into HUVECs containing AMI-Exo or Con-Exo. (**A**) HUVEC proliferation was measured by manual cell counting, CCK8 absorbance (**B**), and EdU staining (**C** and **D**). Scale bar, 50 μm. (**E**) Tube formation analysis of vascular formation ability indicated by tube length (**F**) and node number (**G**). Scale bar, 100 μm. Cells migration was assessed by scratch wound assays (**H**) and analyzed as the ratio of non-migrated area divided by the baseline wound area (**I**). Scale bar, 100 μm. Cell migration was analyzed using Transwell assays (**J** and **K**). Scale bar, 50 μm. (**L**) Microvessels were quantified using aortic sprouting assays (**M**). Scale bar, 200 μm. $^{**}p < 0.01$, $^{***}p < 0.001$.

angiogenesis. The starBase, miRWalk, miRcode, and miRDB databases predicted that TSC1 is a target gene of miR-126-3p (Figure 7A). The qRT-PCR analyses validated that miR-126-3p overexpression greatly suppresses TSC1 expression in HUVECs, with miR-126-3p inhibition exerting the opposite effects (Figure 7B).

To investigate the binding between miR-126-3p and the 3′ UTR of TSC1, we performed luciferase assays in which the TSC1 wild-type 3′ UTR or mutant 3′ UTRs were cloned into a reporter plasmid and their response to miR-126-3p was assessed in HUVECs (Figure 7C). The mimic miR-126-3p markedly decreased luciferase activity, whereas the inhibitor miR-126-3p increased luciferase activity. Moreover, the mutant 3′ UTRs of TSC1 did not alter the response of luciferase activity to the mimic miR-126-3p or inhibitor (Figure 7D). Therefore, these results confirm that TSC1 is a direct target of miR-126-3p.

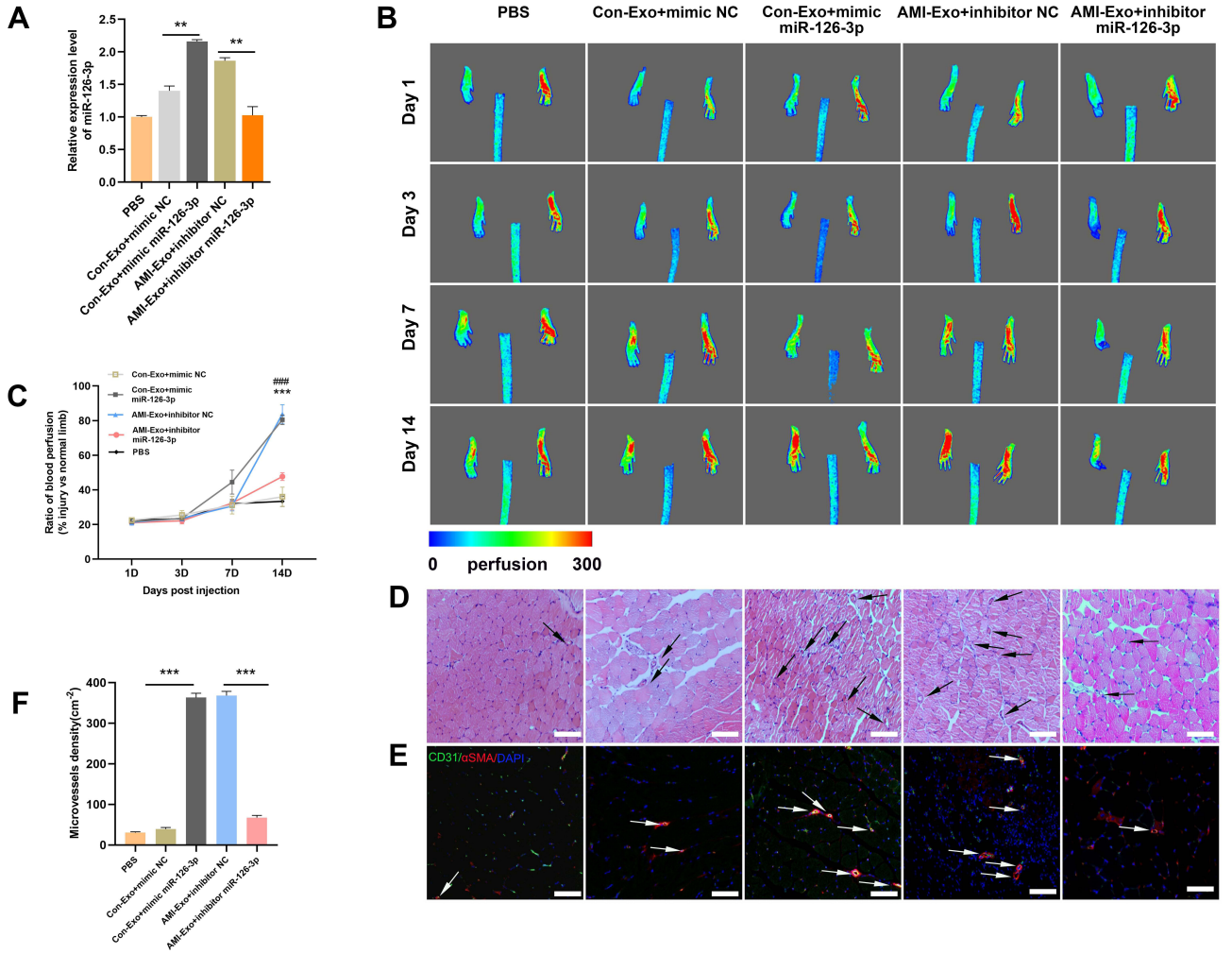

Figure 5 Effect of miR-126-3p in AMI-Exo and Con-Exo on mouse ischemic injury after hind limb ischemia. (**A**) miR-126-3p expression in ischemic muscles was measured using qRT-PCR after treatment for 24 h (n = 3). (**B**) Blood flow perfusion was measured using laser Doppler imaging 1, 3, 7, and 14 days after the exosomes were treated with PBS, mimic miR-126-3p, mimic NC, inhibitor miR-126-3p, or inhibitor NC. The left paw was the ischemic and the right paw was normal control (n = 5). (**C**) The blood perfusion recovery was calculated as the perfusion ratio of the mean velocity in the left rear paw divided by that in the right rear paw. ***Means mimic miR-126-3p vs mimic NC, ###Means inhibitor miR-126-3p vs inhibitor NC (**D**) The gastrocnemius muscle sections were stained by hematoxylin and eosin. (**E**) α-SMA and CD31 were identified based on immunofluorescence (red: α-SMA, green: CD31, blue: DAPI). Arrows indicate microvessels. Scale bar, 100 μm. (**F**) Capillary density in ischemic muscles was measured by the number of microvessels per cm^2. **$p < 0.01$, ***$p < 0.001$, ###$p < 0.001$.

Further Western blot analyses suggested that miR-126-3p overexpression reduces TSC1 expression, with miR-126-3p inhibition boosting TSC1 expression. TSC1 is known to target the mTORC1/HIF-1α pathway.[17] Hence, our next step was to confirm the effects of changes in miR-126-3p expression on the TSC1/mTORC1/HIF-1α pathway. HUVECs treated with mimic of miR-126-3p had improved levels of phosphorylated S6 (pS6) and S6, which are markers of mTORC1 activation, compared to those treated with the control. Conversely, pS6 and S6 levels decreased when the cells were treated with the inhibitor of miR-126-3p. mTORC1 signaling was highly activated in HUVECs along with increase in HIF-1α and VEGFA levels (Figure 7E and F), consistent with previous reports that mTORC1 signaling regulates HIF-1α transcription.[18] Subsequently, we constructed a TSC1 overexpression plasmid and simultaneously transfected with miR-126-3p. We found that the miR-126-3p induced mTORC1 activation and increased the expression of HIF-1α and VEGFA, which were abolished by TSC1 overexpression (Figure 7G and H).

To further investigate whether miR-126-3p could modulate angiogenesis by targeting TSC-1, we utilized validation experiment, wherein, miR-126-3p and TSC1 were overexpressed simultaneously to observe the phenotype of angiogenesis. The overexpression of TSC1 abolished miR-126-3p-promoted endothelial cell proliferation effect, as indicated by CCK8 and Edu analyses (Figure 8A–D). In scratch wound assays, the overexpression of TSC1 could reduce the effect of

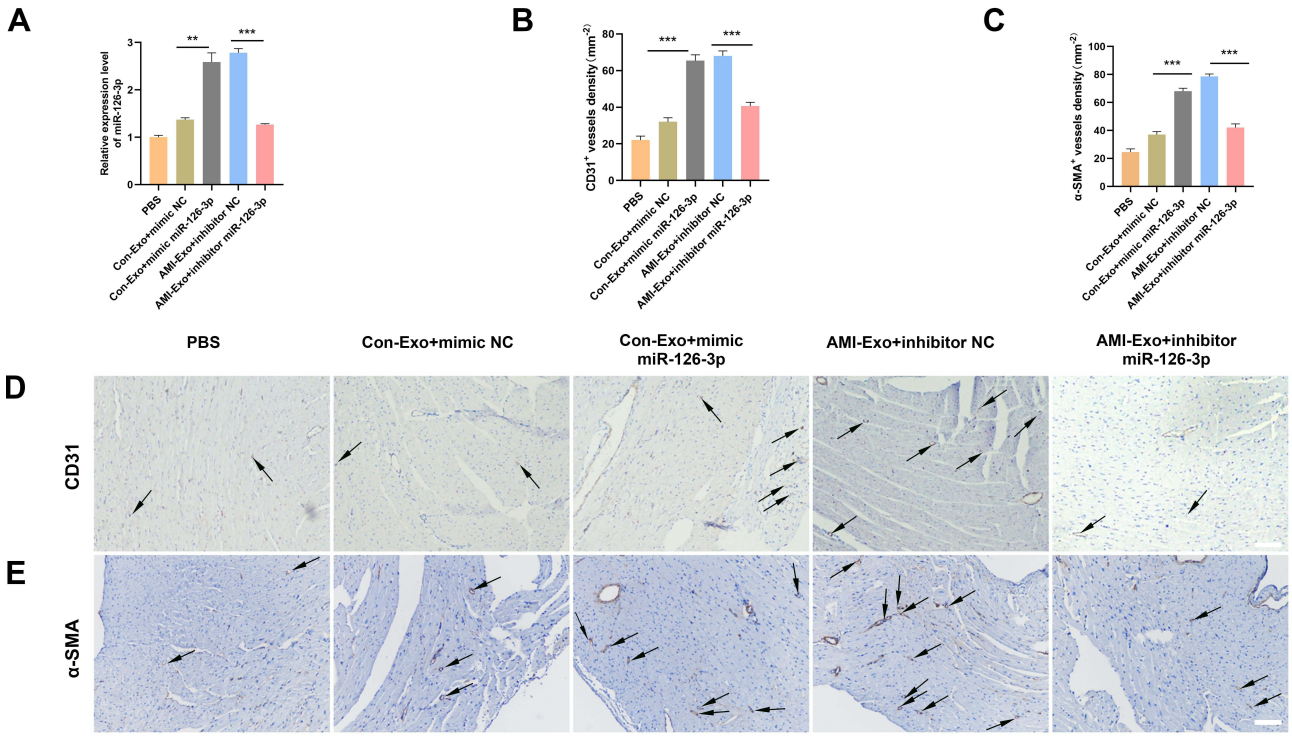

Figure 6 Effect of miR-126-3p in AMI-Exo and Con-Exo on angiogenesis after mouse acute myocardial infarction. (**A**) miR-126-3p expression in ischemic myocardium was measured using qRT-PCR after treatment for 24 h (n = 3). (**B** and **C**) Capillary density in ischemic myocardial was measured by the number of microvessels per mm^2. (**D** and **E**) The CD31 and α-SMA expression was measured using immunohistochemistry. Scale bar, 200 μm. $^{**}p < 0.01$, $^{***}p < 0.001$.

miR-126-3p-promoted cell migration area in wound assay (Figure 8E and F). Furthermore, in aortic ring assay, the overexpression of TSC1 could blocked miR-126-3p induced microvessel sprouting (Figure 8G and H). Collectively, these findings indicate that miR-126-3p promotes endothelial angiogenesis by targeting TSC1.

Discussion

Exosomes carry many functional messages which play key roles in cell-to-cell interactions during myocardial ischemia. MiRNAs are small noncoding RNAs with 22–23 nucleotides that could post-transcriptionally restrain gene expression by targeting the 3′ UTR of mRNAs. Notably, exosomal miRNAs have emerged as key mediators in diverse biological and pathological processes, including the promotion of angiogenesis and improvement of cardiac function.[18,19] Indeed, recent studies have verified that exosomes containing miRNAs can be delivered into other cells to post-transcriptionally regulate gene expression.[20] Exosomes from the coronary artery serum of patients with myocardial ischemia or those with myocardial infarction have been shown to promote angiogenesis through the miR-939-iNOS-NO pathway[5] and through the IGF-IR/NO signaling pathway.[21] However, exosomes secreted by cells may undergo diverse changes and exert different effects under different pathophysiological conditions,[22] and the effects of exosomes derived from the peripheral serum of patients with early stage AMI on angiogenesis remain unclear.

Zhang and Zhang[23] demonstrated that mouse cardiomyocytes could release specific exosomes into the blood-stream under ischemic conditions. Therefore, in this study we obtained exosomes from human peripheral serum, which were subsequently internalized by endothelial cells. We found that AMI-Exo enhanced HUVEC proliferation, tube formation, migration, and enhanced microvessel sprouting from aortic rings. It was recently discovered that exosomes contain numerous miRNAs, including miR-143 and miR-126, that participate in various phases of angiogenesis.[5,15,21] In particular, miR-126 is expressed at high levels in vascular endothelial cells and is known as a master regulator for vascular integrity and physiological angiogenesis.[24,25] Xue et al[26] reported that the expression levels of plasma miR-17-5p, miR-126, and miR-145-3p were significantly augmented in patients with AMI within 4 h of the onset of chest pain. Moreover, Ling et al[27] reported that serum exosomal miR-126 and miR-21 levels were

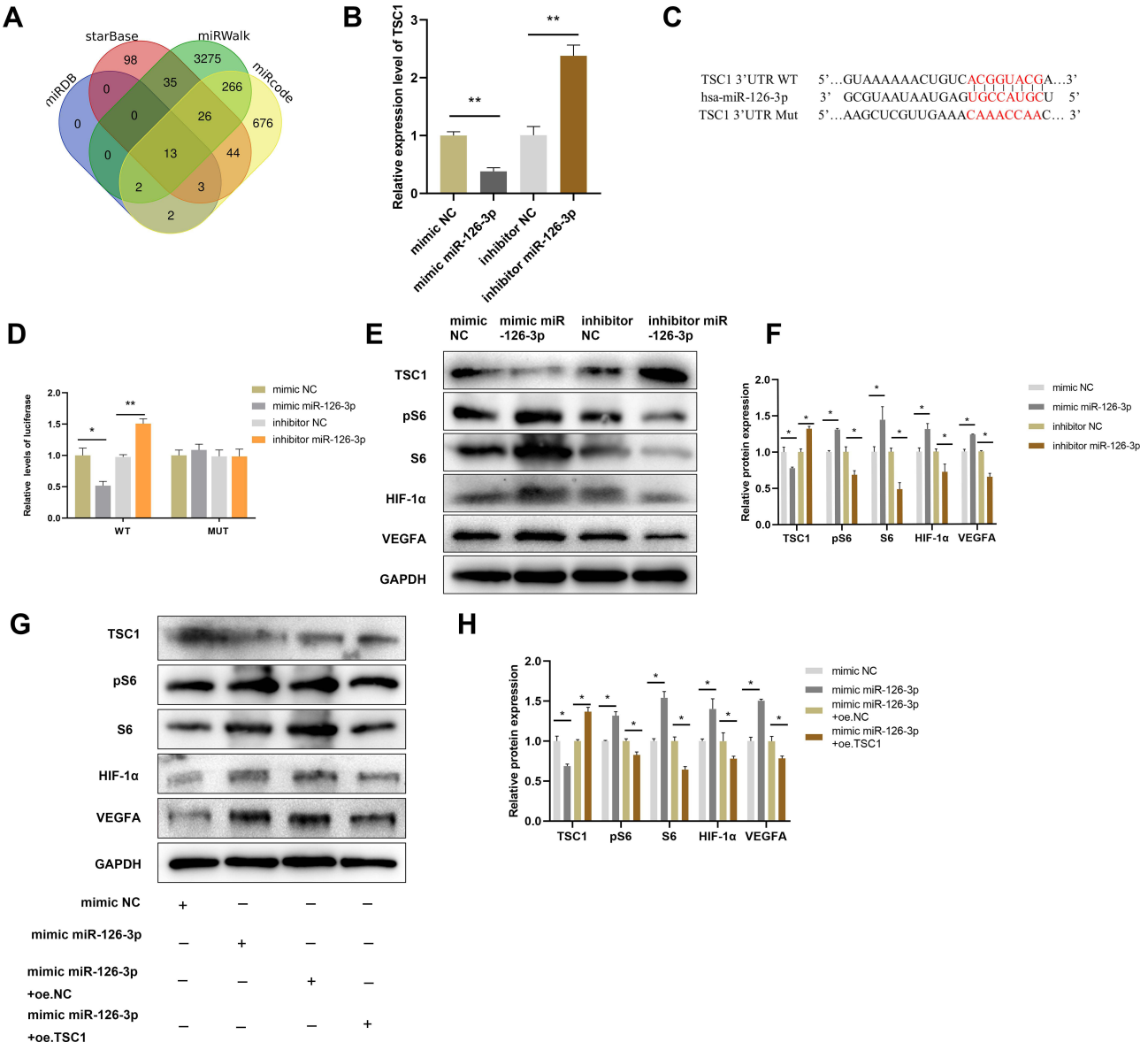

Figure 7 miR-126-3p promotes angiogenesis by directly targeting TSC1. (**A**) Screening miR-126-3p-targeted genes (**B**) Relative mRNA expression of TSC1 in HUVECs after treatment with mimic miR-126-3p, mimic NC, inhibitor miR-126-3p, or inhibitor NC. (**C**) Matched base pairs of the miR-126-3p binding area and reporter plasmids including wild- or mutant-type TSC1. (**D**) Relative luciferase reporter activity of vectors and a fragment of TSC1 UTR with wild- or mutant-type miR-126-3p binding sites after co-transfection with the four groups. (**E**) Western blotting showed the relative protein expression of TSC1, pS6, S6, HIF-1α, and VEGFA in HUVECs treated with the mimic miR-126-3p, mimic NC, inhibitor miR-126-3p, or inhibitor NC. (**F**) Protein expression quantification. (**G**) Western blotting showed the relative protein expression of TSC1, pS6, S6, HIF-1α, and VEGFA in HUVECs treated with the mimic NC, mimic miR-126-3p, mimic miR-126-3p + oe.NC, mimic miR-126-3p + oe.TSC1. (**H**) Protein expression quantification. *$p < 0.05$, **$p < 0.01$.

higher in unstable angina (UA) and AMI patients (within 2 h of AMI) than healthy controls. Moreover, circulating exosomal miR-126 expression levels correlated positively with the severity of coronary artery stenosis defined by Gensini score. Therefore, in this current study, we validated the expression of some angiogenesis-related miRNAs, including miR-143, miR-17-5p, miR-21-5p, miR-939-5p, and miR-126-3p between two groups using qRT-PCR. Among them, the miR-126-3p expression levels were significantly upregulated in AMI-Exo. Moreover, gain-of-function analysis in HUVECs revealed that miR-126-3p significantly promoted cell proliferation, tube formation, migration, and microvessel sprouting. miR-126-3p also improved angiogenesis to a greater extent in AMI-Exo-treated cells than Con-Exo-treated cells in mouse limb ischemia and AMI models.

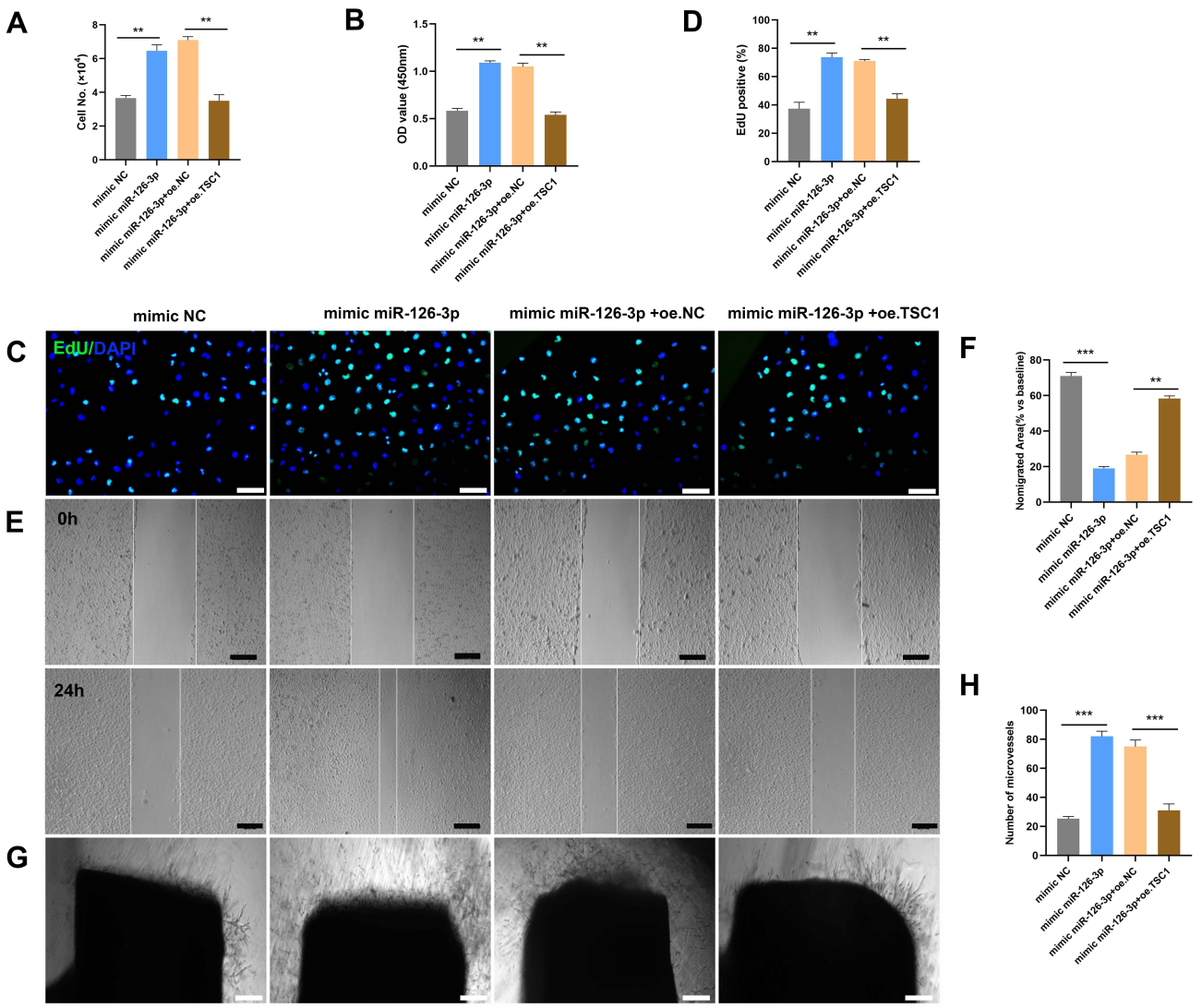

Figure 8 miR-126-3p-targeted TSC1 promotes angiogenesis in vitro. The mimic NC, mimic miR-126-3p, mimic miR-126-3p + oe. NC, and mimic miR-126-3p + oe. TSC1 were transfected into HUVECs. (**A**) HUVEC proliferation was measured by manual cell counting, CCK8 absorbance (**B**), and EdU staining (**C** and **D**). Scale bar, 50 μm. Cell migration was assessed by scratch wound assays (**E**) and analyzed as the ratio of non-migrated area divided by the baseline wound area (**F**). Scale bar, 100 μm. (**G**) Microvessels were quantified using aortic sprouting assays (**H**). Scale bar, 200 μm. $^{**}p < 0.01$, $^{***}p < 0.001$.

Jakob et al[28] previously revealed that exosomal miR-126 from the endothelial cells of patients with chronic heart failure could affect angiogenesis by regulating SPRED1/VEFG signaling. In neonates, TSC1 loss has been shown to increase retinal angiogenesis and lead to endothelial proliferative impairment and generation of vascular tumors in mice by activating mammalian target of rapamycin (mTOR) complex 1 (mTORC1) and increasing HIF-1α and VEGFA expression.[17] Although the post-transcriptional inhibition of TSC1 by miR-126-3p has been reported in granulosa cells,[29] the source and delivery route of miR-126-3p during the early stages of AMI remain unknown. Since bioinformatics analysis and a previous study[29] have hinted that TSC1 is a promising target gene of miR-126-3p, we used luciferase reporter assays to demonstrate that miR-126-3p directly targets the 3′ UTR of TSC1 and represses TSC1 expression.

TSC1 is a subtype of the TSC gene that can form a protein complex with TSC2.[30] The mutations in TSC1 and TSC2 have been shown to give rise to the lymphangioleiomyomatosis.[31] The complex formed by the TSC1 and TSC2 gene products is a pivotal negative regulator of mTORC1 and cell growth.[32] mTOR is a serine/threonine kinase which regulates a number of cellular processes,[33] and any abnormality in mTORC1 signaling can result in many diseases including vascular malformations and even tumors.[34,35] Studies have shown the key role of VEGF in tumor development regulated by HIF-1α,

which is present downstream of mTORC1,[17] and that HIF-1α is an essential mediator of VEGF-induced angiogenesis.[36,37] Consistently, we observed that miR-126-3p targeted TSC1, which activated the mTORC1 signaling pathway, increased pS6 and S6 expression, and increased HIF-1α and VEGFA expression. Interestingly, HIF-1α upregulation has been shown to affect the regulated miR-126 expression upstream that can promote angiogenesis and subsequently improve heart function in myocardial infarction.[38] Therefore, there may be a previously undescribed mechanism underlying the promotion of endothelial angiogenesis that involves a positive feedback loop of miR-126-3p and HIF-1α, and this should be verified in future studies.

Previously, Nie et al[39] reported that circulating miR-126-3p levels were significantly higher in the plasma from sufficient coronary collateral circulation in patients with severely narrowed coronary arteries. Unlike the targeting function of exosomal miRNA, circulating miRNA acts as a rover in the circulatory system that can react with any cell type that is in contact with the blood stream. Therefore, the findings of this study suggest that exosome-mediated miR-126-3p delivery to endothelial cells could better explain the improved coronary collateral circulation in patients with higher miR-126-3p levels.

However, this study also has some limitations. First, we focused on the expression of only few miRNAs in exosomes, which might have resulted in the neglect of other functional miRNAs present in patients with AMI. Second, because of the complicated contents of exosomes, the miR-126-3p/TSC1/mTORC1/HIF-1α pathway may be just one of multiple pathways that regulate angiogenesis.

Conclusion

In summary, our results revealed that miR-126-3p in exosomes derived from the peripheral serum of AMI patients can promote angiogenesis in endothelial cells by targeting TSC1 and activating the mTORC1/ HIF-1α axis. Together, the findings of this study provide a novel understanding of the function of exosomal miRNAs during the early stages of AMI onset.

Ethics Approval and Informed Consent

The research protocol was approved by the Second Affiliated Hospital of Harbin Medical University Ethics Committee (KY2021-147, SYDW2020-030).

We obtained written informed consent from all subjects.

Consent for Publication

We obtained written informed consent from all subjects.

Acknowledgments

We thank the Natural Science Foundation of Inner Mongolia, National Natural Science Foundation of China, and the Fund of Key Laboratory of Myocardial Ischemia, Ministry of Education.

Author Contributions

All authors made substantial contributions to conception and design, acquisition of data, or analysis and interpretation of data; took part in drafting the article or revising it critically for important intellectual content; agreed to submit to the current journal; gave final approval of the version to be published; and agree to be accountable for all aspects of the work.

Funding

This study was financially supported by the Natural Science Foundation of Inner Mongolia [2019MS08148], the National Natural Science Foundation of China [82102068], and the Fund of Key Laboratory of Myocardial Ischemia, Ministry of Education [KF202106].

Disclosure

The authors report no conflicts of interest for this work.

References

1. Virani SS, Alonso A, Aparicio HJ, et al. Heart disease and stroke statistics-2021 update: a report from the American heart association. *Circulation*. 2021;143(8):e254–e743. doi:10.1161/CIR.0000000000000950
2. Zhu W, Sun L, Zhao P, et al. Macrophage migration inhibitory factor facilitates the therapeutic efficacy of mesenchymal stem cells derived exosomes in acute myocardial infarction through upregulating miR-133a-3p. *J Nanobiotechnol*. 2021;19(1):61. doi:10.1186/s12951-021-00808-5
3. Thery C, Witwer KW, Aikawa E, et al. Minimal information for studies of extracellular vesicles 2018 (MISEV2018): a position statement of the International Society for Extracellular Vesicles and update of the MISEV2014 guidelines. *J Extracell Vesicles*. 2018;7(1):1535750. doi:10.1080/20013078.2018.1535750
4. Vicencio JM, Yellon DM, Sivaraman V, et al. Plasma exosomes protect the myocardium from ischemia-reperfusion injury. *J Am Coll Cardiol*. 2015;65(15):1525–1536. doi:10.1016/j.jacc.2015.02.026
5. Li H, Liao Y, Gao L, et al. Coronary serum exosomes derived from patients with myocardial ischemia regulate angiogenesis through the miR-939-mediated nitric oxide signaling pathway. *Theranostics*. 2018;8(8):2079–2093. doi:10.7150/thno.21895
6. Pan Q, Wang Y, Lan Q, et al. Exosomes derived from mesenchymal stem cells ameliorate hypoxia/reoxygenation-injured ECs via transferring microRNA-126. *Stem Cells Int*. 2019:2831756. doi:10.1155/2019/2831756
7. Cao C, Wang B, Tang J, et al. Circulating exosomes repair endothelial cell damage by delivering miR-193a-5p. *J Cell Mol Med*. 2021;25(4):2176–2189. doi:10.1111/jcmm.16202
8. Thygesen K, Alpert JS, Jaffe AS, et al. Third universal definition of myocardial infarction. *J Am Coll Cardiol*. 2012;60(16):1581–1598. doi:10.1016/j.jacc.2012.08.001
9. Thomou T, Mori MA, Dreyfuss JM, et al. Adipose-derived circulating miRNAs regulate gene expression in other tissues. *Nature*. 2017;542(7642):450–455. doi:10.1038/nature21365
10. Zippel N, Ding Y, Fleming I. A modified aortic ring assay to assess angiogenic potential in vitro. *Methods Mol Biol*. 2016;1430:205–219. doi:10.1007/978-1-4939-3628-1_14
11. Melo SA, Luecke LB, Kahlert C, et al. Glypican-1 identifies cancer exosomes and detects early pancreatic cancer. *Nature*. 2015;523(7559):177–182. doi:10.1038/nature14581
12. Tian Y, Li X, Bai C, Yang Z, Zhang L, Luo J. MiR-17-5p promotes the endothelialization of endothelial progenitor cells to facilitate the vascular repair of aneurysm by regulating PTEN-mediated PI3K/AKT/VEGFA pathway. *Cell Cycle*. 2020;19(24):3608–3621. doi:10.1080/15384101.2020.1857958
13. Jin YP, Hu YP, Wu XS, et al. miR-143-3p targeting of ITGA6 suppresses tumour growth and angiogenesis by downregulating PLGF expression via the PI3K/AKT pathway in gallbladder carcinoma. *Cell Death Dis*. 2018;9(2):182. doi:10.1038/s41419-017-0258-2
14. He Q, Ye A, Ye W, et al. Cancer-secreted exosomal miR-21-5p induces angiogenesis and vascular permeability by targeting KRIT1. *Cell Death Dis*. 2021;12(6):576. doi:10.1038/s41419-021-03803-8
15. Mathiyalagan P, Liang Y, Kim D, et al. Angiogenic mechanisms of human CD34(+) stem cell exosomes in the repair of ischemic hindlimb. *Circ Res*. 2017;120(9):1466–1476. doi:10.1161/CIRCRESAHA.116.310557
16. Peter B, Crino KLN, Henske EP. The tuberous sclerosis complex. *N Engl J Med*. 2006;355:1345–1356.
17. Sun S, Chen S, Liu F, et al. Constitutive activation of mTORC1 in endothelial cells leads to the development and progression of lymphangiosarcoma through VEGF autocrine signaling. *Cancer Cell*. 2015;28(6):758–772. doi:10.1016/j.ccell.2015.10.004
18. Kenta Hirai DO, Fukushima Y, Kondo M, et al. Cardiosphere-derived exosomal microRNAs for myocardial repair in pediatric dilated cardiomyopathy. *Sci Transl Med*. 2020;12(573):8764. doi:10.1126/scitranslmed.abb3336
19. Yang H, Zhang H, Ge S, et al. Exosome-derived miR-130a activates angiogenesis in gastric cancer by targeting C-MYB in vascular endothelial cells. *Mol Ther*. 2018;26(10):2466–2475. doi:10.1016/j.ymthe.2018.07.023
20. Meng W, Hao Y, He C, Li L, Zhu G. Exosome-orchestrated hypoxic tumor microenvironment. *Mol Cancer*. 2019;18(1):57. doi:10.1186/s12943-019-0982-6
21. Geng T, Song Z, Xing J, Wang B, Dai S. Exosome derived from coronary serum of patients with myocardial infarction promotes angiogenesis through the miRNA-143/IGF-IR pathway. *Int J Nanomedicine*. 2020;15:2647–2658. doi:10.2147/ijn.S242908
22. McBride JD, Rodriguez-Menocal L, Badiavas EV. Extracellular vesicles as biomarkers and therapeutics in dermatology: a focus on exosomes. *J Invest Dermatol*. 2017;137(8):1622–1629. doi:10.1016/j.jid.2017.04.021
23. Zhang J, Zhang X. Ischaemic preconditioning-induced serum exosomes protect against myocardial ischaemia/reperfusion injury in rats by activating the PI3K/AKT signalling pathway. *Cell Biochem Funct*. 2021;39(2):287–295. doi:10.1002/cbf.3578
24. Wang Y, Sun J, Kahaleh B. Epigenetic down-regulation of microRNA-126 in scleroderma endothelial cells is associated with impaired responses to VEGF and defective angiogenesis. *J Cell Mol Med*. 2021;25(14):7078–7088. doi:10.1111/jcmm.16727
25. Zhou Q, Anderson C, Hanus J, et al. Strand and cell type-specific function of microRNA-126 in angiogenesis. *Mol Ther*. 2016;24(10):1823–1835. doi:10.1038/mt.2016.108
26. Xue S, Liu D, Zhu W, et al. Circulating MiR-17-5p, MiR-126-5p and MiR-145-3p are novel biomarkers for diagnosis of acute myocardial infarction. *Front Physiol*. 2019;10:123. doi:10.3389/fphys.2019.00123
27. Ling H, Guo Z, Shi Y, Zhang L, Song C. Serum exosomal MicroRNA-21, MicroRNA-126, and PTEN are novel biomarkers for diagnosis of acute coronary syndrome. *Front Physiol*. 2020;11:654. doi:10.3389/fphys.2020.00654
28. Jakob P, Doerries C, Briand S, et al. Loss of angiomiR-126 and 130a in angiogenic early outgrowth cells from patients with chronic heart failure: role for impaired in vivo neovascularization and cardiac repair capacity. *Circulation*. 2012;126(25):2962–2975. doi:10.1161/CIRCULATIONAHA.112.093906
29. Yuan X, Deng X, Zhou X, et al. MiR-126-3p promotes the cell proliferation and inhibits the cell apoptosis by targeting TSC1 in the porcine granulosa cells. *Vitro Cell Dev Biol Anim*. 2018;54(10):715–724. doi:10.1007/s11626-018-0292-0

30. Marjon van Slegtenhorst MN, Nagelkerken B, Cheadle J, Snell R. Interaction between hamartin and tuberin, the TSC1 and TSC2 gene products. *Hum Mol Genet*. 1998;7(6):1053–1057. doi:10.1093/hmg/7.6.1053
31. Huang J, Wu S, Wu CL, Manning BD. Signaling events downstream of mammalian target of rapamycin complex 2 are attenuated in cells and tumors deficient for the tuberous sclerosis complex tumor suppressors. *Cancer Res*. 2009;69(15):6107–6114. doi:10.1158/0008-5472.CAN-09-0975
32. Nisreen El-Hashemite VW, Zhang H, Kwiatkowski DJ. Loss of Tsc1 or Tsc2 induces vascular endothelial growth factor production through mammalian target of rapamycin. *Cancer Res*. 2003;63:5173–5177.
33. Foster KG, Fingar DC. Mammalian target of rapamycin (mTOR): conducting the cellular signaling symphony. *J Biol Chem*. 2010;285 (19):14071–14077. doi:10.1074/jbc.R109.094003
34. Du W, Gerald D, Perruzzi CA, et al. Vascular tumors have increased p70 S6-kinase activation and are inhibited by topical rapamycin. *Lab Invest*. 2013;93(10):1115–1127. doi:10.1038/labinvest.2013.98
35. Shirazi F, Cohen C, Fried L, Arbiser JL. Mammalian target of rapamycin (mTOR) is activated in cutaneous vascular malformations in vivo. *Lymphat Res Biol*. 2007;5(4):233–236. doi:10.1089/lrb.2007.1012
36. Rattner A, Williams J, Nathans J. Roles of HIFs and VEGF in angiogenesis in the retina and brain. *J Clin Invest*. 2019;129(9):3807–3820. doi:10.1172/JCI126655
37. Tian X, Liu Y, Wang Z, Wu S. miR-144 delivered by nasopharyngeal carcinoma-derived EVs stimulates angiogenesis through the FBXW7/HIF-1α/VEGF-A axis. *Mol Therapy*. 2021;24:1000–1011. doi:10.1016/j.omtn.2021.03.016
38. Song W, Liang Q, Cai M, Tian Z. HIF-1alpha-induced up-regulation of microRNA-126 contributes to the effectiveness of exercise training on myocardial angiogenesis in myocardial infarction rats. *J Cell Mol Med*. 2020;24(22):12970–12979. doi:10.1111/jcmm.15892
39. Xiaomin Nie LS, Zhou Y, Zhao Y. Association between plasma levels of microRNA-126 and coronary collaterals in patients with coronary artery disease. *Chin J Cardiol*. 2014;42(7):561–565.